

**MARTIAN SOUTHERN HEMISPHERE DEBRIS APRONS.** H. Li, M. S. Robinson, and D. M. Jurday, Northwestern University (Department of Geological Sciences, 1850 Campus Dr., Evanston, IL 60208, USA (han@earth.northwestern.edu, robinson@earth.northwestern.edu, donna@earth.northwestern.edu).

**Introduction:** Debris aprons, lobate-shaped ice-related thick deposits have been identified in the mid- to high-latitude range of both hemispheres of Mars [1,2,3,4,5]. [6] reported the differences in surface morphologies and morphometric characteristics of aprons between several regions in the northern and southern hemispheres. We surveyed the southern debris aprons, specifically aprons near eastern Hellas region, centered at (40°S, 106°E) to understand their topographic and morphometric nature. By comparing the topographic characteristics of the southern and northern aprons, we seek to understand whether similar apron development mechanisms have taken place in these two hemispheres with large elevational, geological, and climatic differences.

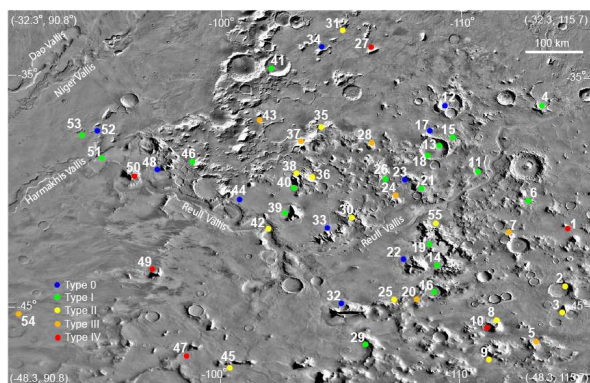


Fig 1: Distribution of eastern Hellas region debris aprons.

**Background:** Aprons in the southern hemisphere are emplaced on the higher, more heavily cratered highlands, although the southern aprons exhibit similar surface ages as the northern ones. In the southern hemisphere, [7] identified >90 debris apron complexes throughout the Promethei Terra region to the east of the Hellas basin. Within Promethei Terra region, aprons are particularly common in the Reull Vallis and Harmakhis Vallis area, where [8] catalogued 54 apron complexes, each composed of a single apron or, more commonly, a coalesced mass of multiple aprons with a common source. These aprons belong to the Amazonian period, and most are eroded from Noachian aged massifs or the basin rim unit, with the rest associated with Hesperian or Amazonian-Hesperian material [9].

**Data and Methods:** We identified 50 single aprons with MOLA profiles passing at right angle to the apparent flow direction (Fig. 1), a subset of the 54 previously catalogued apron complexes. These aprons are distributed in the latitudinal band of 47°S to 33°S, within longitudes 109°E-

115°E. We measured the horizontal length, thickness, and elevation of each apron by extracting the section of MOLA profile that passes across the feature. Multiple MOLA profiles were used for accuracy when available. We then compared the longitudinal profile of aprons with ice sheet profiles predicted by simple plastic and viscous power law models, two models often used to study terrestrial glaciers and ice sheets. Detailed description of the models can be found in [5, 10].

**Results:** The average size of studied debris aprons is 0.28 km thick by 6.7 km long, with thickness and length values ranging from 0.030-0.9 km and 1.3–22 km, respectively. The median elevation where studied aprons emplaced is measured to be  $0.468 \pm 1.434$  km. Emplaced at elevations about 6 km higher than those in the north, eastern Hellas region aprons are smaller in size for a single flow, however, they tend to coalesce to form large apron complexes.

When normalized to unit length and thickness, the profiles of the eastern Hellas aprons exhibit an overall convex trend with several aprons deviating to concave shapes (Fig. 2). We quantitatively classified the aprons by comparing each deposit's longitudinal profile with the simple plastic model. Details of this classification can be found in [5]. The results are shown in Table I.

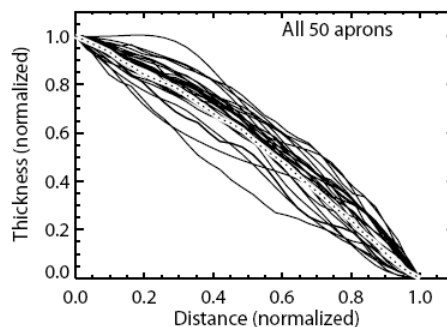


Fig. 2: Profiles of eastern Hellas aprons, normalized to unit length and thickness. Dotted line = median profile.

Type	Number	Length (km)	Thickness (km)	H/L (? $10^{-3}$ )
0	9	9.5	0.259	27
I	15	4.6	0.239	52
II	15	7.1	0.332	47
III	8	4.0	0.281	71
IV	3	6.9	0.279	41

Table I: Summary of eastern Hellas apron trends.

We also compared the five types of southern hemisphere aprons by normalizing them based on mass or

volume conservation (Figure 3). From type 0 through type IV, the median profiles not only become progressively less convex, their horizontal lengths also increase monotonically to accommodate this change. Type I through IV volume-normalized composite profiles cross the simple plastic model at the lower slope of the apron and reach out further horizontally. In contrast, type 0 composite profile does not reach horizontally as far as the simple plastic model, but exceeds the maximum length the of viscous power law model.

**Discussion:** As in the northern hemisphere [5], we did not find any correlation between apron type and the elevation or poleward orientation of aprons. Type 0 aprons exhibit the lowest thickness/length ration, which is consistent with the assumption that they have the highest ice content.

Representing an ice sheet's initial unstable stage and the final stable stage after readjustment, respectively, the viscous model and simple plastic model can be taken as two snapshots in the development of an ice sheet, before and after it stabilizes. Type 0, plotting between the two models (Fig. 3), very likely represents a transitional stage of development in the aforementioned adjustment process, i.e. a debris-covered ice-rich body deforms towards a mechanically more stable state.

**Conclusions:** Debris aprons in the eastern Hellas basin differ from their northern counterparts in distribution, morphometric measurements, and topographic characteristics. In the southern hemisphere, a new type of aprons, type 0, with the most convex profile and rising above the simple plastic model, were identified. The new type 0 aprons are suggestive of a different stage of apron development that is not observed in the North. This type may represent an ice-rich deposit still going through viscous deformation towards a more stable, plasticity state. The identification of geologically young and possibly active debris aprons in the Eastern Hellas region suggest that the erosion of ancient Noachian-aged terrain in the southern hemisphere likely to be an ongoing process. Debris apron formation is especially prominent in regions with large elevation differences and where ground ice is present to facilitate the process.

**References:** [1] Squyres, S. W. (1978) *Icarus*, 34, 600-613. [2] Squyres, S. W. (1979) *JGR*, 84, 8087-8096. [3] Lucchitta, B. K. (1984) *JGR*, 89, 409-418. [4] Mangold, N. and P. Allemand (2001) *GRL*, 28, 3, 407-410. [5] Li, H. et al., (2005) *Icarus*, 176, 382-394. [6] Chuang, F. and D. Crown (2005) *Icarus*. [7] Crown, D. et al. (2002) LPS XXXIII, Abstract #1642. [8] Pierce, T.L. and D. Crown (2003) *Icarus*, 163, 46-65. [9] Mest, S.C. and D. Crown (2001) *Icarus*, 183,

89-100. [10] Li, H. et al. (2004) *LPS XXXV*, Abstract #2120.

**Acknowledgements:** We thank Northwestern Boos Fellowship for supporting this research.

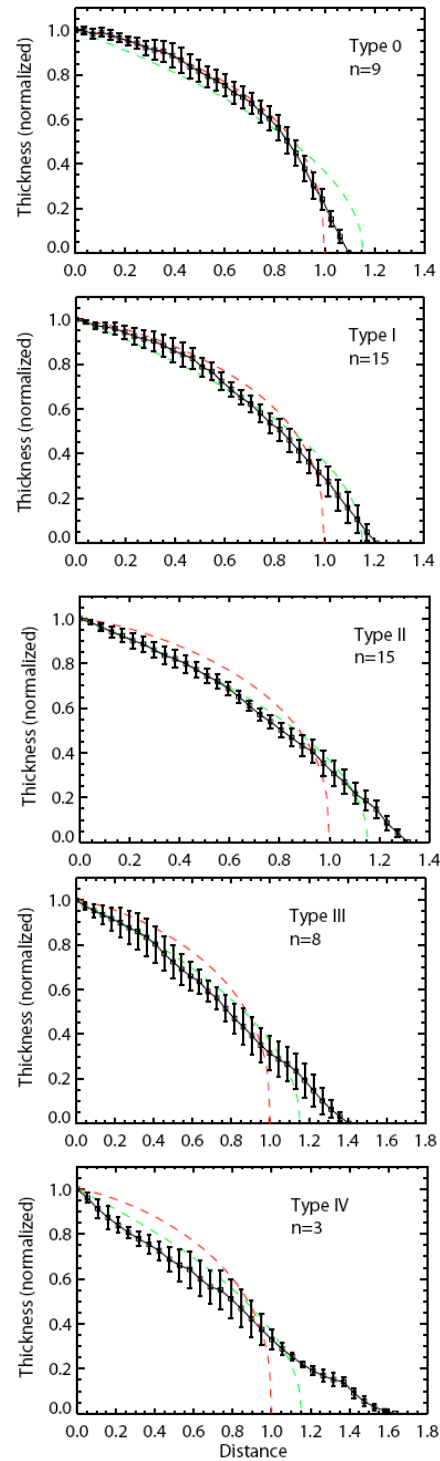


Fig. 3: Volume-normalized composite profiles of type 0-IV aprons. Upper red dotted line = viscous power law model; lower green dotted line = simple plastic model.